

# Predicting complex user behavior from CDR based social networks

Casey Doyle<sup>a</sup>, Zala Herga<sup>b,c</sup>, Stephen Dipple<sup>a</sup>, Boleslaw K. Szymanski<sup>a,d,\*</sup>,  
Gyorgy Korniss<sup>a</sup>, Dunja Mladenić<sup>b,c</sup>

<sup>a</sup>*Rensselaer Polytechnic Institute, 110 8th Street, Troy, NY 12180, USA*

<sup>b</sup>*Jožef Stefan Institute, Jamova 39, Ljubljana, Slovenia*

<sup>c</sup>*Jožef Stefan International Postgraduate School, Jamova 39, Ljubljana, Slovenia*

<sup>d</sup>*Spółeczna Akademia Nauk, Łódź, Poland*

---

## Abstract

Call Detail Record (CDR) datasets provide enough information about personal interactions to support building and analyzing detailed empirical social networks. We take one such dataset and describe the various ways of using it to create a true social network in spite of the highly noisy data source. We use the resulting network to predict each individual's likelihood to default on payments for the network services, a complex behavior that involves a combination of social, economic, and legal considerations. We use a large number of features extracted from the network to build a model for predicting which users will default. By analyzing the relative contributions of features, we choose their best performing subsets ranging in size from small to medium. Features based on the number of close ties maintained by a user performed better than those derived from user's geographical location. The paper contributions include systematic impact analysis that the number of calls cutoff has on the properties of the network derived from CDR, and a methodology for building complex behavior models by creating very large sets of diverse features and systematically choosing those which perform best for the final model.

*Keywords:* social networks; complex behavior prediction; probability of default; feature selection; Call Detail Record dataset

---

\*Corresponding author

*Email address:* [szymab@rpi.edu](mailto:szymab@rpi.edu) (Boleslaw K. Szymanski)

---

## 1. Introduction

Call Detail Record (CDR) datasets, created from cell phone logs of large groups of people, have become common in studying human behavior thanks to the large amount of detailed data they provide [10]. These datasets typically include both basic information about the users (age, gender, location) as well as event records for calls and text messages detailing the time, location, and direction of the communication. This information provides a bird’s-eye view of human interactions without the self-reporting bias inherent to many other behavioral studies, allowing for observations and predictions on behavior such as payment reliability. It also enables researchers to work with otherwise prohibitively large sample sizes and to study subtle relationships between various aspects of the user’s behavior.

Here, we analyze such a dataset and focus on the properties of the underlying social network that can be obtained from the data. First, we discuss various methods for building the network, aiming to mitigate the noise inherent within the cell phone records and address other issues identified in prior work such as the definitions of links, communities, reciprocity, and data types suitable for the study. These considerations are particularly relevant to our application due to the large amounts of noise and potential biases inherent to various network representation schemes [35, 41, 51, 38, 71]. We analyze how does the number of calls cutoff impact the properties of the network derived from CDR focusing on a balance between noise reduction and loss of information within the resulting network. Using the analysis results, we build two networks to mitigate the above mentioned pitfalls during collecting two different sets of features.

Early studies of CDR datasets relied upon individual location data to investigate the very basic correlations [79]. Since then, higher level statistics are used to study complex behavior, including considerations of social groups and socio-economic status [47, 62]. In particular, modern studies have investigated the relative socio-economic status of geographic regions using factors such as

the total volume of calls, while others have concentrated on predicting social attributes via personal mobility and social network centrality [44, 19, 60, 23]. In this paper, we combine these techniques by using basic geographic and usage features along with higher level social network measures such as centrality and community structure to predict the probability of individuals defaulting on their accounts.

The specific CDR dataset used here includes the detailed call history of 500,000 clients of a cell phone company over a three month period. The dataset contains also information about the users' basic demographic data (age, home district, gender, and default status at the end of the three month period) as well as usage information (frequency and duration of calls, messages, and movement records based on frequently used cell towers). We perform traditional network analysis on the data to create new complex features. In particular, we focus on the social network that can be constructed from the contact records between users, building a graph of the relationships and analyzing user behavior. One contribution of our paper is the systematic analysis of the impact that the cutoff for the number of calls needed to create an edge in the network has on the properties of the network derived from CDR. Based on this analysis, we first use a frequency cutoff at which the network is stable to define an unweighted edges that identify basic relationships between individuals. Then, we switch to a weighted representation to ascertain information on the paths between individuals and to investigate reciprocity imbalances among users.

We use the default status (an indicator of whether the client stopped paying the phone bill over the course of data collection) as the predicted variable. It is typically accessible as a part of the user's phone records, yet it still measures a complex user behavior combining many different behavioral factors. The combination of a financial burden competing with social and moral obligations makes this feature useful for comparing different regions where purely wealth-centric measures may be difficult to standardize across cultures.

To encompass the wide variety of possible correlations between individual attributes, behavioral indicators as well as network metrics and the probabil-

ity of default, we create extremely broad features set, aggregating thousands of features from all the facets of information contained in the CDR dataset. Then, we perform feature contribution analysis and choose the features with the strongest predictive power to balance model performance and its complexity. As discussed in the next section, this general methodology for building complex behavior models is a novel approach and our contribution to the state of the art.

## **2. Related work on modeling complex human behavior**

### *2.1. Personality traits and complex user behavior*

Researchers have been working on identifying a person’s personality from non-standard sources (mobile phones, speech, video) for more than a decade now, especially since smart phones and social platforms emerged making rich behavioral data easily available. Personality studies are frequently based on the Big-Five Personality traits [18, 20, 14, 5]. These traits define five factors commonly used to describe the human personality and psyche: openness to experience, conscientiousness, extroversion, agreeableness, and neuroticism. Typical research for this group of papers was presented in [20] that aims at inferring people’s personality traits based on their phone call behavior. The study included 39 people, each characterized with self-reported Big-Five traits and 474 features derived from phone usage logs. Support Vector Machine (SVM) regression used to process this data yielded Mean Square Error (MSE) from 0.73 to 0.86. More in-depth analysis presented in [14] has shown that each trait has specific communication behaviors correlated with it.

Newer research in this area tends to focus on complex online user behavior, such as website visits [26], social media [45, 37, 42], intelligent games [63], (improving) recommender systems [55, 77, 40, 76, 39, 53, 50], web spam behavior [2, 48], and signature verification [21]. One study aimed at predicting the team formation for class projects based on the students’ social media (Facebook) networking data [12].

Understanding complex user behavior is also important for commerce. Customer behavior is analyzed in this context via the web data mining, especially web mining for E-commerce [28]. Another approach, segmentation [15], categorizes customers into groups based on their similar behaviors. This enables the businesses to selectively target the customers with product offerings matching their needs.

A lot of research was done to enable prediction of user’s future behavior for marketing, including predicting whether user is going to buy [11, 43], lose interest [73, 25] or default on company’s products of services [58, 1]. Our paper contributes a new methodology for the last problem, specifically predicting the default on a user’s cell phone bill.

## *2.2. Mobile phone data*

With the rise of smart phones a lot of research has been done using data collected from mobile phones. Mobile phone usage data (e.g., variation in usage, periodicity of usage) was chosen as a base for predicting loan repayment in [9]. The results enabled the participating banks to reduce defaults by 41% while accepting 75% applications for loans. In other works, call logs, locations, and proximity to others (bluetooth scans) together with self-reported data were used to infer social network structure [22] and its evolution [7]. In another study, 26 couples allowed for tracing their social interaction patterns (proximity, call, sms) and self-reported their spending, which enabled the authors to build a predictive model of participants’ spending behavior [61].

Call detail records (CDR) is a standard dataset collected by telecom operators. For each user, it contains information about telecommunication events in which this user was involved. In recent years, it has become a popular source of information for users’ behavioral analytics. Other types of data (e.g. demographic, Big-Five questionnaire, credit default reports) are also used for modeling the collective behavior of a population [59], calling patterns [29], predicting personality [18, 20], telecom attrition [27], socioeconomic levels [64], credit defaults [58] etc. The authors of the last paper on this list built a model of the

user’s financial risk which yields a score that can be interpreted as the probability of default. Their model outperforms the Credit Bureau scores by using thousands of weak predictors derived from CDR and demographic data.

### *2.3. Credit risk management*

Our paper focuses on credit risk, which refers to the clients who may stop paying back their loans, e.g., mortgage loan, credit card spending or phone bill. Such events are called defaults. Banks and companies traditionally tackle this problem by calculating credit scores or probability of default for each of the potential clients. In case of the corporate clients, the most commonly used data is financial and macroeconomic indicators, e.g., [65], while some studies have taken into account less standard data like corporate governance characteristics [16].

Unlike enterprises, which prepare financial statements every year, consumers usually do not offer a lot of financial data, especially younger people and first time borrowers. To overcome this issue, creditors and researchers started using alternative data sets to predict a customer’s probability of default, like demographic data, loan and credit information [6], social media [24, 78] or mobile phone data [9].

Traditionally, the logistic model was often used to predict defaults and today is still useful for benchmarking thanks to its simplicity, interpretability and dependability [72, 6, 33]. However, more sophisticated and innovative approaches are also used (at least in research), like neural networks [72, 78, 34], smart ubiquitous data mining [6], theory of three-way decisions [46], and theory of survival [33]. In our paper, we introduce a novel approach that starts with creating a large number of features (over 6,000 here) and then reducing them to a few well performing subsets.

## **3. Network Creation and Analysis**

In this section, we define the node-level location and communication activity features that indicate how embedded the node is in the network which deter-

mines the cost of leaving the network. Such social network analysis is common in working with CDR datasets [10], but the highly detailed information contained in the CDR comes with a large amount of noise. Quantifying what level of communication between individuals indicates a connection is challenging. This issue is made worse considering the potential bias introduced by specific patterns of communication, as generational and cultural divides are prominent in phone usage [41]. Therefore use of case-specific methods is common. Some attempts at a more general solution to this problem include reciprocity or activity requirements for links, but these solutions suffer from losing many fine details of the system [35]. More complete results can be obtained by using statistical methods to detect and remove links that are more likely to be random, but the methods come with increased computation cost [38].

In this study, we address these problems through the lens of our relatively narrow focus on building a social map of how information flows between users. For detailed analysis, we use directed graphs in order to preserve the imbalances that tend to arise even among reciprocal relationships [32]. We also use communication frequency between individuals to define edges. For simpler metrics, we use unweighted graphs. For a more complex metrics, we use a weighted graph explicitly represent the paths between individuals and reciprocity imbalances among users. While the resulting graph is inherently noisier than the unweighted one, it also represents better relationship strength and network location properties.

### *3.1. Unweighted network with frequency cutoff*

We define the unweighted network via a cutoff,  $c$ , representing the minimum number of communications from node  $i$  to node  $j$  required for an edge to be drawn [49]. Specifically, if you consider the weight of communications between node  $i$  and node  $j$  to be the total volume of communications  $w_{i,j}$ , then the condition for a directional link being formed from node  $i$  to node  $j$  is  $w_{i,j} \geq c$ . This link then becomes an unweighted directional edge from node  $i$  to node  $j$  without restricting the possibility of another link forming from node  $j$  to node  $i$

to create an unweighted bidirectional edge. One main advantage of constructing the network in this way is that it allows the network to be simplified, removing noise while still retaining information regarding the frequency of communication. Still, the methodology proposed here contains some inherent loss of information partially stemming from the use of the raw number of communications between individuals. To account for possible differences in the amount of information contained in calls versus texts, it is natural to attempt to use different communication weights based on communication type. As such, we experimented with such methods to better account for these information exchange levels and found that any such scheme would cause bias between age groups. In general, since younger individuals used more text messages while older individuals used more calls we treat their contributions to the network flatly to minimize bias.

This method yields a strict structural view of the true friendship network, addressing the need for noise reduction by pruning down the network as well as showing how robust the network is to increasingly strict friendship requirements. In Fig. 1(a), we show that the giant component of the network decays exponentially with an increased frequency cutoff for edges, and is generally very sensitive to such an increase. Without a cutoff, the giant component of the network contains 99.1% of the nodes, but it drops to only half of the network when the frequency cutoff reaches 30. A similar effect can be seen in Fig.1(b), where the total number of edges in the social network shows a power law decay for increasing cutoff values. This power law decay of edges implies that the scheme is useful for removing noisy, low frequency communication while leaving intact the dense communications representative of strong social ties. The proper cutoff value for a given situation is difficult to establish, however, since the vast majority of connections in the network are low frequency. In fact, less than half of the original edges remain when a cutoff of  $c = 4$  is implemented. As the cutoff increases further, the network loses much of its connectivity and instead shows a rough sketch of the community structure of the system. This effect is seen in Fig. 1(c), in which the percentage of nodes outside of the giant component that are isolated *decreases* with increased cutoff, the result of

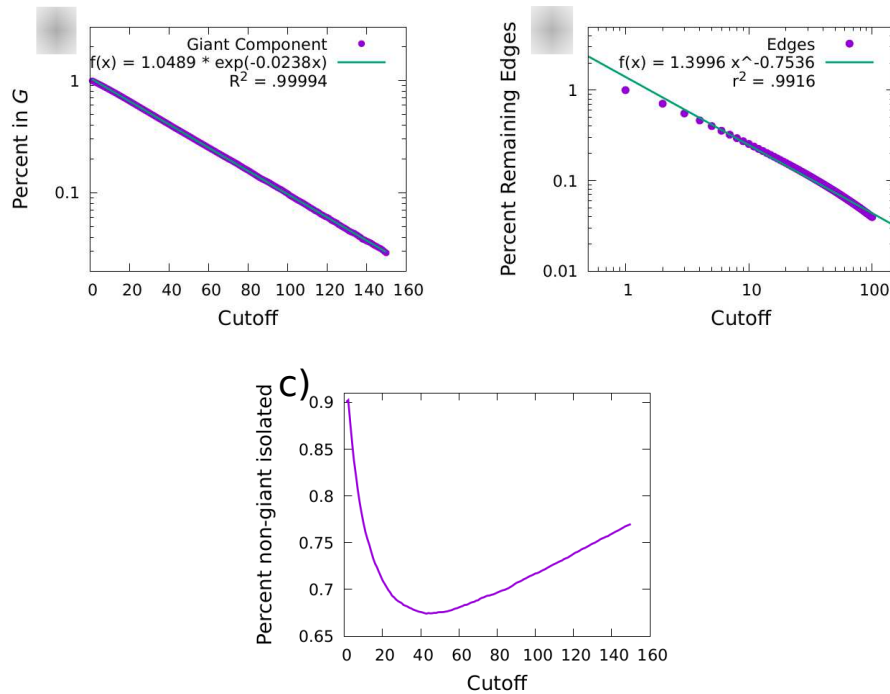


Figure 1: (a) The giant component of the social network decays exponentially ( $\lambda = 0.0238$ ) with increased minimum number of communications required for an edge to be drawn. (b) The number edges in the network also decays rapidly with increased cutoff, closely fitting a power law with  $\gamma = 0.7536$ . (c) The percentage of non-giant component nodes that are isolated for a given cutoff. The isolated nodes reach a minimum at a cutoff of 43.

small communities being separated from the giant component but remaining intra-connected. Of course, these results yield only a crude approximation of the community structure; high cutoffs lower the connectivity within communities as well as separate them from the giant component. This trade-off becomes apparent at cutoffs larger than  $c = 43$ , where the number of isolated nodes increases and even tightly bound communities unravel. A more direct and robust detection of the network’s community structure is discussed in Sec. 3.3.

In addition to the effects on the connectivity of the network, the frequency cutoff also has a significant impact on the overall degree distribution (shown in Fig. 2). As expected [38, 51, 8], for all values of the cutoff the degree distribution shows a power law tail. However, the rate at which the tail decays changes as the

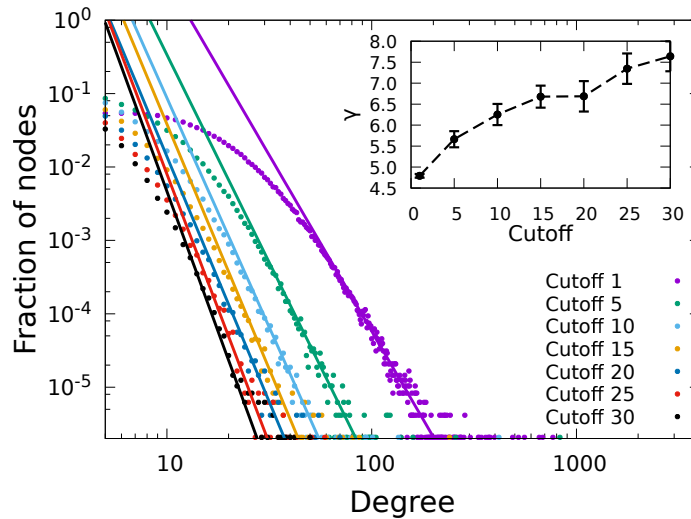


Figure 2: The out-degree distribution of the mobile phone network for various edge weight cutoffs. The inset shows the estimated power law exponent for the various cutoff values to highlight the different scaling rates.

edges are removed. As the cutoff increases, many of the highest degree nodes lose the vast majority of their edges. As a result, the higher cutoffs greatly reduce the maximum degree of the network and increase the power scaling exponent of the degree distribution causing faster tail decay [3, 31, 17]. As with the prior results on increased cutoff, however, this is only true to a point. The exponent increase appears to saturate at high values of the cutoff where the impact gets weaker and weaker. These properties allow us to use an unweighted graph with low cutoffs to define basic network features such as node degree, while higher cutoff values are useful for finding the stable number of strong contacts.

### 3.2. Weighted network based on event frequency

While using a cutoff scheme is effective for determining the giant component stability and degree distribution, it lacks valuable information that can be used to better understand other details within the network. For these more in-depth network features, we must turn to traditional methods of analyzing networks that require weighting and distancing information for the edges. For this pur-

pose, we build a weighted network such that if  $w_{i,j} > 0$ , a directed link is formed from node  $i$  to node  $j$  with weight  $w_{i,j}$ .

This scheme is particularly useful for metrics that use distance-based calculations (diameter, centrality, some forms of community detection), allowing us to account for the reduced ‘distance’ between two heavily connected nodes. For all such distance-based applications, we use a link’s weight to define a normalized distance from the source node  $i$  to the target node  $j$ , defined as  $d_{i,j} = w_{avg}/w_{i,j}$  where  $w_{avg}$  is the average weight of all connections in the network. The higher noise in the system from not using the cutoff reduction scheme is minimized in these calculations through the nature of the distance measure. Since in shortest path calculations it is highly unlikely that a short path will run through an extremely sparse communication, the sparse edges are not used unless they are the only possible route from one node to another. Finally, to provide a baseline with which we can compare the network to, we also rewire the network by swapping the edge destinations to create a pseudo-random weighted graph that maintains the in and out-degree structure of the original network.

We first look at the measure of harmonic closeness centrality (closeness centrality adapted to non-connected graphs) [57, 52]. It indicates how critical a node is to the various pathways through the network. This metric is defined as  $C_H(i) = \frac{1}{N-1} \sum_{j \neq i} \frac{1}{l_{i,j}}$ , where  $N$  is the total number of nodes and  $l_{i,j}$  is the distance of the shortest path between nodes  $i$  and  $j$ . For the cell network, these centrality scores are generally fairly high and evenly distributed, with an average harmonic centrality of  $C_{avg}^{cell} = 4.61$  and a standard deviation of  $C_{std}^{cell} = 1.84$ . Both values are higher than those for the randomly rewired graph which yields  $C_{avg}^{rand} = 4.11$  and  $C_{std}^{rand} = 1.20$ . Interestingly, the diameter and average shortest path length of the giant component in the cell network  $D^{cell} = 6.24$  and  $\langle l^{cell} \rangle = .311$  are also slightly higher than the corresponding values  $D^{rand} = 4.35$  and  $\langle l^{rand} \rangle = .30$  for the randomly rewired network. These differences reveal the basic shape of the cell network, which is characterized by significant populations of both highly connected and highly isolated nodes. This property can be interpreted from the high centrality and standard devia-

tion of the cell phone network, but is shown more clearly via the diameters of the two networks. The cell phone network is significantly wider, as despite the existence of close communities and hubs within the network, there are multiple extremely remote nodes with no close ties. This information can be used to identify how deeply embedded a node is within the network, an important concept for predicting the nodes most at risk for defaulting or leaving the network in the future.

Further, this weighted network provides greater detail for other common network statistics such as the reciprocity [71]. Even with just the unweighted version of the network, the surprisingly low reciprocity of the network is apparent with only 62.88% of links having communications in both directions. Further investigation using the edge weights, though, allows us to study reciprocity on a deeper level for use as a node-level feature set. We construct our reciprocity metric to be the average contribution of a nodes' links so that it is independent of the degree of the node. In addition we require this metric to exist for nodes with directional links as opposed to [71]. To this end, we define reciprocity as  $R_i = \frac{1}{k_i} \sum_{j \in N(i)} \frac{w_{i,j} - w_{j,i}}{w_{i,j} + w_{j,i}}$ , where  $k_i$  is the total (both in and out) degree of node  $i$ ,  $w_{i,j}$  is the number of communications from node  $i$  to node  $j$ , and  $N(i)$  is the set of neighbors that have a link connected to node  $i$ . Using this definition, links over which a node is sending more than receiving contribute positively to the node's metric, while links with the reverse pattern contribute negatively. Additionally, the absolute value of the contribution itself increases monotonically with the difference in the level of communication [71]. Finally in order to compare each link on equal footing, every link's contributions are bound within the range [-1,1].

We show in Fig 3(a) that the distribution of these reciprocity scores is fairly smooth with large spikes at the extreme values. These spikes are created by nodes with either no incoming communications ( $R_i = 1$ ) or no outgoing communications ( $R_i = -1$ ), and can be partially explained as a relic of the dataset. Since all data comes from a single cell phone provider, it is likely that many of these nodes simply have contacts that use different carriers not included in

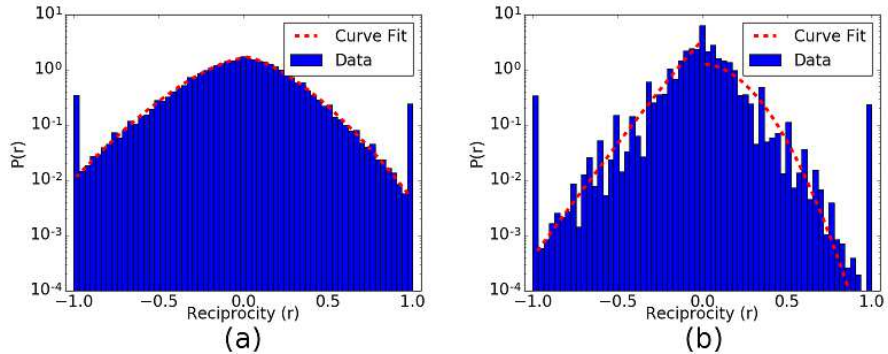


Figure 3: a) The distribution of reciprocities. (b) The distribution of reciprocities using a randomized network. Peaks are observed at -1, and 1. This is consistent with a large number of nodes have low degree as most links are not reciprocated. The randomized network produces a narrower and rougher distribution indicating some level of order in how individuals interact.

the set. Removing these outliers, we fit the remaining distribution using the equation  $f(x) = Ae^{-x^B/C}$  where  $A$  normalizes the values,  $B$  controls the curvature, and  $C$  determines the width of the distribution. Table 1 shows the fitting parameters for Fig 3. As can be seen, there is an asymmetry in the width of the positive and negative side of the distribution. This can be caused by an increased amount of communication for nodes with reciprocity equal to 1. While each link's contribution  $w_{i,j} - w_{j,i}$  is symmetric, the overall contributions are averaged and thus the symmetry can be broken. If an unreciprocated link is the only link for a node, its reciprocity will be  $R_i = \pm 1$  regardless of what  $w$  is. This means if there are overall more communications from nodes with  $R_i = 1$  than nodes with  $R_i = -1$ , this difference would show itself in the overall distribution.

Next, we examine the distribution of reciprocities when the links are randomized (Fig 3(b)). Compared to Fig 3(a), the concavity of the distribution narrows from the presence of more frequent values close to zero. Hence, the empirical network derived from the phone records is more diverse than a similar random graph would be. Moreover, the directionality and volume of calls between pairs of individuals are important in defining their usage patterns, and thus provide a valuable new network feature for our predictive analysis.

Fitting Parameter	CDR Graph		Random Graph	
	Positive	Negative	Positive	Negative
A	0.547	0.477	0.236	1.21
B	1.52	1.49	1.96	1.07
C	0.168	0.198	0.080	0.111
$R^2$	0.994	0.991	0.687	.961

Table 1: The fitting parameters used in Fig 3. Positive and Negative refer to the fit of the distribution where the reciprocity values are positive and negative respectively. Due to the non-integer value of the curvature, we fit the absolute value of the negative side and plot accordingly. For the CDR graph both positive and negative sides have very similar fitting parameters except for the width in the distribution which suggest an asymmetry.

For other possible representations of reciprocity within the network, see Appendix A, where we discuss two additional variants that can mathematically produce similar results to introducing a cutoff but without loss of information. These alternative metrics are however not independent from the metric presented in this section, and thus are not suitable as independent features. The presented metric is used here for its simplicity without significant loss of information.

### 3.3. Community detection and geographical districts

Finally, the weighted directed network allows us to analyze more deeply the social communities present in the system. To this end, we use the GANXiS(SLPA) algorithm for its ability to detect even disjointed and overlapping communities and fully encapsulate the social structure of the network. GANXiS(SLPA) is a speaker-listener label propagation technique that allows membership in multiple communities at once and is optimized for extremely large networks [75, 74], making it ideal for this application. Using this algorithm we identify a set of over 6450 social communities, many more than the 231 geographic communities derived from the districts reported. Despite the size differences (the largest district contains 63491 users while the largest social community has just 741 with an average of only 74.65 users), the groups are substantial enough to test the

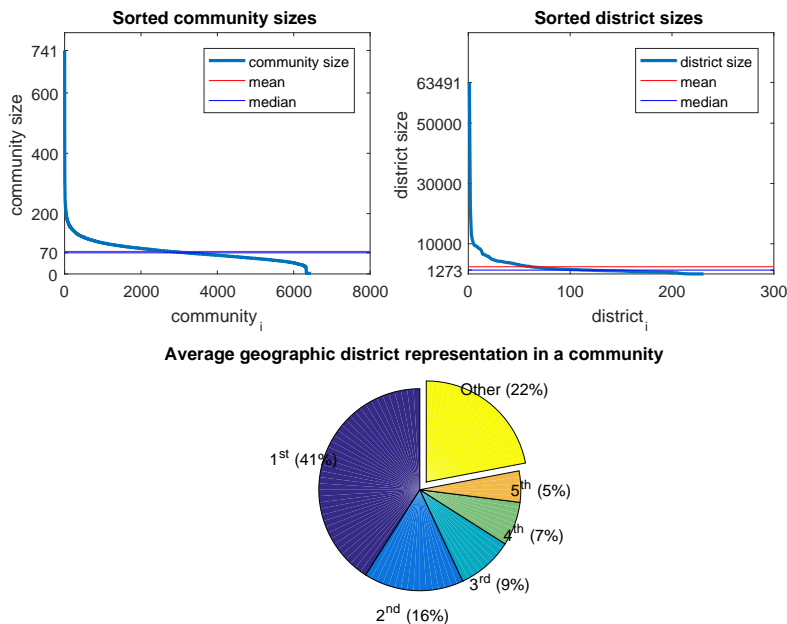


Figure 4: Top: Community and districts sizes, which are sorted in descending order. The average social community size is 75 with a median of 70, whereas geographic districts show an average of 2,380 and median of 1273. Bottom: average proportion of users from a community that belong to the same geographic district - from most represented geographic district by users (1<sup>st</sup>) to the 5<sup>th</sup> most represented.

overlap of the lists for greater insight into how the social ties form. Intuitively, it seems that the social communities are highly influenced by the geographic district of their members, but instead we see in Fig. 4 that on average only 41% of each community comes from the same district, and in fact even the top five districts only account for 78% of each community's makeup. The diversity of the geographic locations within social groups is especially surprising given the generally small size of the social groups compared to the geographic districts.

#### 4. Feature Generation

We combine the above described network features with the various raw usage and location features that are inherent to the dataset to create our full feature set. For ease of analysis, we divide them into six groups:

1. **High Level Network features** - explained in detail above. This subset consists of 5 features.
2. **Consumption features** - includes information about the total number of communication events, the total and average duration of phone calls, and average time between consecutive communications. This subset consists of 2784 features.
3. **Correspondent features** - based on the distinct number of individuals that each user communicates with over various time periods. This subset consists of 2561 features.
4. **Reciprocated event features** - number of events where the observed user returns a call/message within a specified time period of receiving a communication. This subset consists of 672 features.
5. **Mobility features** - includes the movement patterns of individuals based on the cell tower used for each communication with relation to commonly used towers. This subset consists of 29 features.
6. **Location features** - includes the two most used cell phone towers for each user. This subset consists of 2 features.

In some cases large or very inclusive features can be broken up by analyzing time windows (hours, days, day of the week, weeks, months, business hours, non-business hours, weekend, weekday), direction (ingoing/outgoing event), and communication type (call/message), leading to a large overall set of more than 6000 features. Most of these features are standard, so we do not present them in detail here, but relegate the full descriptions of each feature set to Appendix B.

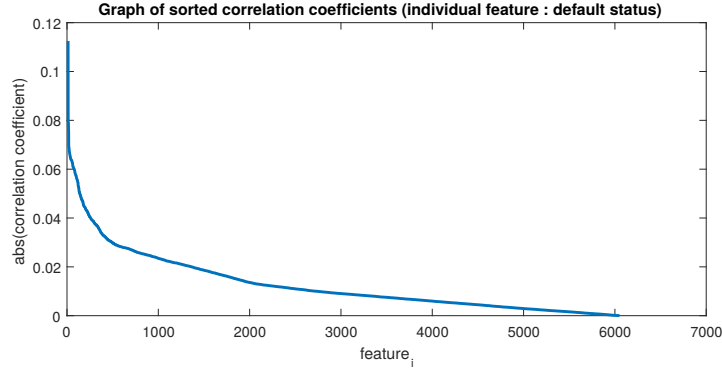


Figure 5: This graph shows point biserial correlation of each individual feature to default status. Values are sorted in descending order by absolute value of their correlation coefficient. Features with highest absolute correlation (originally all negative) are the average number of used cell towers in one week, distance traveled in a day of week and the average daily radius.

## 5. Predicting default status

### 5.1. Correlation analysis

We utilize point biserial correlation to define the basic correlation between each feature and user default status due to its suitability for handling both categorical and continuous variables as are present in our feature set. This process indicates that individual features tend to have very little correlation to default status (shown in Fig. 5), with a maximum absolute correlation of only 0.1155 and average correlation of  $-0.006$ . This poor individual correlation shows that no single feature reproduces the default status of the individuals reliably, proving the value of building an accurate predictive model through more complex analysis.

### 5.2. Modeling

#### 5.2.1. Logistic regression

To create the predictive models, we start by defining the logistic regression

$$P(Y) = \frac{1}{1 + \exp^{-\beta_0 - \beta X}}, \quad (1)$$

where  $Y$  is the dependent variable vector of length  $n$ ,  $X$  is a matrix of size  $n \times p$  with rows corresponding to observations and columns to predictor variables (features),  $\beta$  is a vector of regression coefficients of length  $p$ , and  $P(Y)$  is the probability of “success” (in our case default).

From this base, we fit several models with varying parameters, starting with a model that uses only 7 features: 5 network measures and 2 location features. They provide a high level view of individual behavior and intuitively may be expected to contain stronger signals than many other features. With so few features, we implement this model simply with no preceding feature space reduction. This solution obtains  $p$ -values  $\leq 0.01$  for all features except for duration, which has a  $p$ -value of 0.97. Thus, all six features (excluding duration) are good predictors for default status.

### 5.2.2. *Principal Component Analysis*

To build a more complex model that utilizes the other 6048 features, we first normalize the features to mean values of 0 and variance 1. Once normalized, to deal with the extremely large number of features we perform Principal Component Analysis [54](PCA) to decompose the feature space and yield a set of “principal components”. The results are linearly uncorrelated and ranked in such a way that the first principal component explains the highest possible amount of variability in the data, while each following component explains the highest amount of variance under the condition that it is orthogonal to all preceding components. Once these components are obtained, we select subsets of the components that account for large amounts of variability in the data and use them as explanatory variables for a linear model. We do this for both large and small subsets of the components, as pruning the data in this way represents a careful balance between model simplicity and accuracy. In our dataset, this balance manifests in the rapidly diminishing returns seen from larger component inclusion. The first component explains 20% of variability in the data while the second explains only 7%. In fact, the first thirty components together explain only 42% of the variability, while the first five hundred sum up to just 66%. For

this reason, we generate two distinct logistic models: a simple one based on the first 30 PCA components (*pca-30*) and a more complex one, based on the first 500 PCA components (*pca-500*). We use notation  $p_1$  for the number of selected principal components. We then map our features into the new space to fit these groupings, such that

$$X_{PC} = X \cdot C,$$

where  $C \in \mathbb{R}^{p \times p_1}$  is the matrix of  $p_1$  principal components and  $X_{PC} \in \mathbb{R}^{n \times p_1}$  is the new feature matrix. Finally, we also fit a model (*pval-05*) using only those variables from *pca-500* that have a  $p$ -value  $< 0.5$  to include the greater detail of the larger model with a lower complexity for calculation.

### 5.2.3. Other models

We further examine the data by utilizing other techniques, and build models for each as a comparison to the above described PCA models. For instance, one large issue with our dataset is that positive samples (defaulted users) account for only 0.25% of the whole dataset, making it extremely unbalanced. Learning from this kind of unbalanced dataset is a well-known challenge in the data mining community that we attempt to account for by performing oversampling (multiplying positive samples to make them a larger portion of the dataset) [13]. In this case, we use multiplication factors ranging from 2 – 100, but in the model benchmarks presented here, we show only the model with a multiplication factor of 2 (*oversampled-2*) since it performed the best. Oversampling was applied to the reduced dataset ( $X_{PC}$ ).

Further, as an alternative to the PCA reduction presented in the prior section, we also build a separate model by selecting features via Lasso regression [69]. This method adds a penalty term to the log likelihood function in the prediction that shrinks the coefficients of less important variables to zero. We fine tune this reduction via a free parameter  $\lambda$ , varying it through a range of values to obtain the best lasso fits. The efficacy of this method is demonstrated in two separate models: one based on logistic regression (*lasso-logistic*) and another using a Support Vector Machine [70] (*lasso-svm*).

Finally, the last model we use for comparison utilizes a simple method for feature space reduction that aggregates some of the more specific features into general descriptions of behavior. For instance, features that were based on a particular day or week of the three month period are grouped and combined, creating instead features for weekdays versus weekend averages or business hours versus off-hours. This aggregation not only simplifies the model, but also makes it generalizable to other datasets with different levels of detail. This method shrinks the overall feature set considerably, leaving only 781 features. As before, these features are then normalized before being further reduced via PCA.

## 6. Results and Discussion

### 6.1. Experimental setting

After each of the above models is fit to a training set comprising 70% of the whole dataset, they are tested on the remaining 30% of the data and evaluated via their recall, fall-out, and precision. Defaulting users are labeled as positive examples and default predictions are defined as those users within the 95<sup>th</sup> percentile of default probabilities. This threshold is chosen to be relatively low to fit the nature of our study where false positives (non-defaulted users that were predicted as defaulters) are less damaging than false negatives (unidentified defaulters) to companies.

The recall (the true positive rate) is the rate of identified defaulting customers. The fall-out (the false positive rate) is the probability of labeling a good client as a defaulting one. The precision is the fraction of correct default predictions out of all default predictions. These metrics are calculated as

$$recall = \frac{TP}{TP + FN}, \quad fall-out = \frac{FP}{FP + TN}, \quad precision = \frac{TP}{TP + FP}$$

where TP is the number of true positives, FN is the number of false negatives, FP is the number of false positive, and TN is the number of true negatives.

## 6.2. Evaluation

The performance of the models tested can be compared using a receiver operating characteristic curve (ROC), which we show in Figure 6. Here, we focus this comparison on the recall and fall-out of the model, where recall (which identifies defaulting customers) is of interest to phone companies, while fallout has greater relevancy in other applications of the models. The exact values of these performance metrics can be seen in Table 2, which also shows the precision of each model for reference.

The initial results are in line with what would be expected intuitively: the worst performance comes from the random model, followed by *glm-7* (the logistic model based on only 7 features). As the models become more complicated, their performance tends to increase. For instance, a significant reduction in false positives can be seen in the *lasso-logistic model* (which uses 309 variables) over the *glm-7*, then a further reduction in the *lasso-svm* model that uses 475 variables. Additionally in both Lasso models, the variable with the highest coefficient is the user’s most commonly utilized cell tower, indicating the presence of geographic regions which are high risk areas for user defaults. Other high performance models include the various PCA models, led by *pca-500*, *pval-05* and *oversampled-2* with *pval-05* outperforming all other models.

From these results, it is clear that for the most part larger feature sets allow for more accurate models (as would be expected), but this is not a strict rule. The best performing model is the one that begins with a large sample of features, but is then stripped of those that aren’t considered significant. In other words, there are likely some ‘false flags’ in the feature list that tend to confuse the model rather than contribute. Feature removal only works to a point, however, as the more aggressive methods in the *pca-aggr* model lose these benefits and in fact make it one of the worst performing models tested. Thus, there is likely some very meaningful information even within the extremely specific features that would be intuitively too limited to contribute much. Finally, it should be noted that while the highest performing oversampling model, *oversampled-2* yields improvements comparable to filtering insignificant features, applying

both techniques *worsens* the results as the model apparently over-fits.

Model	Recall	Fall-out	Precision
random	0.060	0.0501	0.003
glm-7	0.224	0.0495	0.012
lasso-logistic	0.484	0.0490	0.023
pca-aggr	0.676	0.0484	0.036
lasso-svm	0.749	0.0482	0.040
pca-30	0.810	0.0480	0.043
pca-500	0.889	0.0478	0.047
oversampled-2	0.897	0.0478	0.047
pval-05	0.900	0.0477	0.048

Table 2: Recall, fall-out and precision for each of the models presented in Figure 6. Precision is low due to the fact that the dataset is majorly unbalanced; however, precision of the best model is about 15 times higher than in the random model.

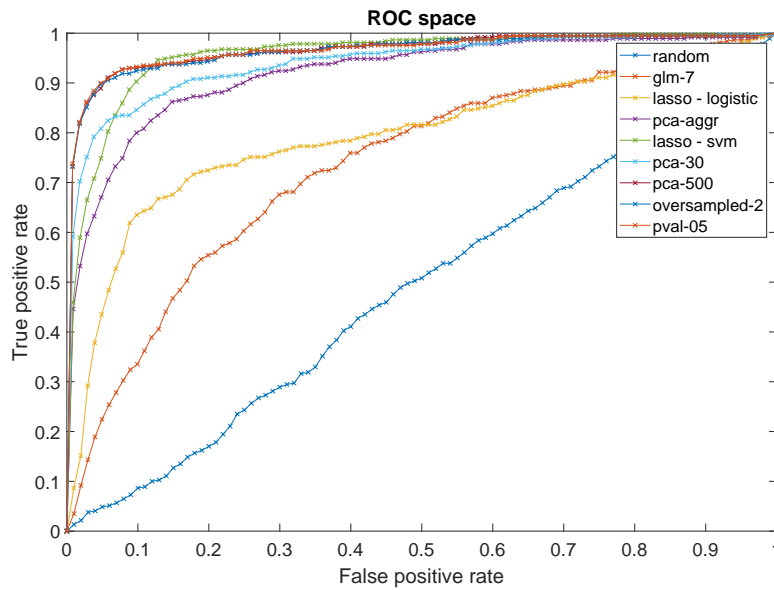


Figure 6: Model performance when predicting defaulting users from worst to best: *glm-7*, *lasso-logistic*, *pca-aggr*, *lasso-svm*, *pca-30*, *oversampled-2*, *pca-500* and *pval-500*.

### 6.3. Stability

For a more in depth look into the differences in prediction among the top three models (*oversampled-2*, *pca-500*, *pval-05*), we look at the overlap size (the intersection of correctly labeled defaulting customers) and average overlap score (the similarity of two rankings at increasing depth giving higher weights to higher ranked observations; AOS). All analysis is restricted to only those customers with a calculated probability of default (PD) in the 95 – *th* quantile. As can be seen in Table 3, both the overlap and AOS are extremely high for all model comparisons, indicating that all three models are stable and predict roughly the same nodes for default. Further, the *pval-05* and *pca-500* models can be seen to be more similar to each other than the *oversampled-2* model due to *pval-05* being essentially *pca-500* with some of the problematic features removed.

		pval-05	pca-500	oversampled-2
pval-05	overlap	100	98.8	97.3
	AOS	100	96.5	94.3
pca-500	overlap		100	97.9
	AOS		100	95.5
oversampled-2	overlap			100
	AOS			100

Table 3: Overlap size (in percentage) and average overlap score of correctly labeled defaulting customers for the three best models.

### 6.4. Contribution of feature sets

Finally, we identify the original features that contribute the most to our models to gain a better understanding of what aspects of the mobile phone data are most important for predicting default status. However, as we mentioned before in Sec. 5.1, each feature is generally fairly poorly correlated with defaults. Thus it is no surprise that there is no one outstanding feature that stands out as the strongest contributor. To remedy this, we perform a general analysis using

Model	RECALL	PRECISION	$\Delta$ Recall	$\Delta$ Precision
Full feature set	0.9	0.048	-	-
- consumption f.	0.88	0.047	0.02	0.001
- correspondent f.	0.58	0.031	0.32	0.017
- reciprocated f.	0.88	0.046	0.02	0.002
- mobility f.	0.88	0.046	0.02	0.002
- network f.	0.88	0.05	0.02	-0.002
- cell tower PD f.	0.89	0.050	0.01	-0.002
Only correspondent f.	0.86	0.049	-	-

Table 4: Results of models based on reduced feature sets. In each row, the underlying dataset is missing one category of features (listed in first column of the table). Two models that proved to be the best were fitted in each case: *glm-500* and *glm-500-filt*. Most features contribute only about 2-3% to the final recall and 0.1-0.2% to the final precision, except for correspondent features which contribute 33% of recall and 1.9% of precision.

the feature set groupings described in Sec. 4 to identify which class of features contributes the most. By building a host of modified models, each consisting of all of the feature sets except one, we can compare the performance of the models with the reduced data against the model with all data included. This method allows us to gain a better understanding of how much information is lost when a feature set is removed (i.e. how unique that information is), data that is especially valuable to this study considering the high redundancy in our data set.

As shown in Table 4, by far the highest contributors to recall and precision are the correspondent features, which focus on individual’s unique frequent correspondents in various time frames. To better understand exactly what features within the correspondent feature set are important, we perform 5-fold cross validation on a linear model using only these features. On average, this model is able to achieve a 0.86 recall and 0.049 precision, both fairly high for such a small subsection of the features. Further, we explore which out of the 2543 correspondent features contribute most to the final PD by mapping the maximum

likelihood estimation (MLE) coefficients of PCA components back to original features' coefficients,

$$\hat{\beta} = C \cdot \hat{\beta}_{PC}$$

where  $\hat{\beta} \in \mathbb{R}^{2543 \times 1}$ ,  $C \in \mathbb{R}^{2543 \times 500}$  is the matrix of principal components and  $\hat{\beta}_{PC} \in \mathbb{R}^{500 \times 1}$  are the MLE coefficients for a model fitted on 500 PCA components.

We then multiply each regression coefficient by the mean of the corresponding feature (separately for paying and defaulting customers). Finally, we define a score for each user based on the values of  $\hat{\beta}X_j$ ,  $j = 1, \dots, n$ . This creates a system where higher scores correspond to customers with higher PD's, and leads to an average score of  $-0.0453$  for paying customers and  $16.2758$  for defaulting customers. This analysis is not possible using the whole feature set together, as the normalization of the features leads to an average contribution of zero, but the absolute contribution values of each feature are taken into account to maintain a focus on the actual impact of the features on the PD. The results for the four strongest features are presented in Table 5. In the end, the same ten features are identified as the strongest contributors for both the paying and defaulting customer groups. All ten relate to the number of unique correspondents with whom the user communicates during the holiday period around Christmas and New Year's Eve. This strongly indicates a tie between not only unique correspondents and defaulting, but also unique correspondents around holiday periods (when users are most likely to be contacting close family and friends). From these results we can begin to draw a clear connection of low probability of default with the large number of active unique ties an individual has within the network, and the high strength of those ties.

However, it should be noted that this kind of estimation of variable contribution is too simple to provide a definitive insight into the relative importance of the variables. There are several other approaches that compare predictors in regression including methods considering variable importance via  $R^2$  partitions [56, 67], dominance analysis [4] and relative weights analysis [30, 36].

Feature	Mean relative contribution
unique message correspondents (12/24)	0.043
unique message correspondents (incoming, 12/24)	0.041
unique message correspondents (outgoing, 12/24)	0.024
unique correspondents (outgoing, 12/24)	0.023
sum	0.131

Table 5: Four features with the highest contribution to the PD calculated on separate sets of paying and defaulting customers. All of the top 10 relate to the number of unique correspondents during holiday period around Christmas and New Year’s Eve.

According to the literature, the dominance analysis provides the most accurate results, but it is not practical for our problem since it measures relative importance in a pairwise fashion and is suitable only for small variable sets. Instead, the relative weights approach is sometimes used for systems with multiple correlated predictors as can be found here [36], but this approach is theoretically flawed and is therefore not recommended for use [68]. We instead utilize a variable importance (VI) extension for logistic regression [67] that is based on Pratt’s axiomatic [56] and the geometric approach of Thomas [66]. This method equates VI to variance explained by the variable, which is  $\beta_j \rho_j$ , where  $\beta_j$  is the standardized regression coefficient and  $\rho_j$  is the simple correlation between variables  $Y$  and  $X_j$ . For our purposes, we use the geometric approach to this method; an interpretation of Pratt’s measure based on the geometry of least squares. Here, the VI indices are defined as

$$d_j = \frac{\hat{\beta}_j \hat{\rho}_j}{R^2}, j = 1, \dots, p, \quad (2)$$

where hats denote sample estimates, and  $R^2$  is as usual the proportion of sample variance explained.

Further, we utilize a pseudo- $R^2$  measure based on Weighted Least Squares such that this set of indices sums to one and the importance of a subset of variables is equal to the sum of their individual importance. This results in the four most important features, according to VI metric, shown in Table 6,

Feature	$d_j$
unique message correspondents (12/24)	0.048
unique message correspondents (incoming, 12/24)	0.045
unique message correspondents (outgoing, 12/24)	0.029
unique correspondents (outgoing, 12/24)	0.026
sum	0.148

Table 6: Ten features with the highest contribution to the PD. All of them relate to the number of unique correspondents during holiday period around Christmas and New Year’s Eve.

yielding results very similar to the ones presented in Table 5. The two most important variables are: the number of unique correspondents with whom the user had a call on Dec 24th with relative importance of 0.048, and the number of unique correspondents from which the user received a message on Dec 24th with relative importance of 0.045. This finding reiterates the significance of the number of unique correspondents with whom the user communicates around holiday periods. Finally, to ensure that these features actually carry unique information, we fit another model removing from the dataset the features with the highest identified VI. Doing so reduces the recall by 0.042 and leaves none of the new identified important variables with a relative importance above 0.03.

## 7. Conclusion

In this paper, we investigate many different aspects of user behavior to build a large suite of features for analysis, starting with constructing the underlying social networks based on the cell phone usage data. Accordingly, our first contribution is the systematic analysis of the impact that a cutoff of the number of calls for creating an edge has on the properties of the network derived from CDR. Based on this analysis we used two different networks for obtaining needed information. First, we define an event frequency cutoff that balances the need for reducing noise from the system while preserving the information critical to computing the features when creating the corresponding unweighted graph. For

more complex features that require higher detail, we create a weighted graph that retains most of the useful information at the cost of higher noisiness.

The complex nature of default status leads us to utilize a large set of over 6000 initial features, which we then pare down to only the most predictive ones. This novel approach is another contribution of our paper to the state of the art. The resulting model achieves a recall of 0.9 with a fall-out of only 0.048, the performance that compares favorably with [58, 1], e.g., recall of 0.674 is reported in the later reference.

Finally by investigating in depth the various features that contribute to the model, we are able to pinpoint the overwhelmingly best, and surprising, contributor: the number of unique contacts with whom the user interacted around the winter holidays (when users are most likely to contact their closest friends and family). The significance of this correspondent information is higher than that of more traditionally mined features demonstrating the need for systematic approach to selecting features for complex behavior prediction. Indeed, our results show that the strength of links within the network is better determined by the timing of communications rather than the volume, duration, or distance traditionally used for the similar predictions.

While our use of CDR data here focuses on user analytics and predictive modeling, CDR datasets can support many other avenues of research. This work investigates the default status of individuals, but there are many other complex aspects of user behavior that could benefit from similar computational techniques. Further, while the various noise reduction techniques are shown to be very destructive to the network’s overall structure, they leave a core set of communications surviving even when high information loss methods are implemented. A more thorough look at these resilient edges could give a clearer idea of exactly which relationships are strongest against this type of noise reduction technique. Additionally, a deeper look at the edge removal’s effects on the clustering and communities within the network could lead to a better understanding of the network structure. On the predictive side, the modeling we present could be improved by gathering information over larger time periods in order to get

a larger population of defaulting individuals. And finally, with new machine learning algorithms constantly being designed and improved, a more specific algorithm that is built for high dimensional data such as ours could improve the resultant predictions and understanding of how the specific features contribute to the overall model.

## 8. Acknowledgments

Funding: This work was supported in part by the Army Research Laboratory (ARL) under Cooperative Agreement Number W911NF-09-2-0053 (NS-CTA), by the Office of Naval Research (ONR) Grant No. N00014-15-1-2640, and by RENOIR EU H2020 project under the Marie Skłodowska-Curie Grant Agreement No. 691152. The views and conclusions contained in this document are those of the authors and should not be interpreted as representing the official policies either expressed or implied of the Army Research Laboratory or the U.S. Government.

## References

### References

- [1] Agarwal, R. R., Lin, C.-C., Chen, K.-T., and Singh, V. K. (2018). Predicting financial trouble using call data—on social capital, phone logs, and financial trouble. *PloS one*, 13(3):e0191863.
- [2] Al-Kabi, M. N., Alsmadi, I. M., and Wahsheh, H. A. (2015). Evaluation of spam impact on arabic websites popularity. *Journal of King Saud University-Computer and Information Sciences*, 27(2):222–229.
- [3] Alstott, J., Bullmore, E., and Plenz, D. (2014). powerlaw: A Python Package for Analysis of Heavy-Tailed Distributions. *PLoS ONE*, 9(1):e85777.
- [4] Azen, R. and Budescu, D. V. (2003). The dominance analysis approach for comparing predictors in multiple regression. *Psychological methods*, 8(2):129.

- [5] Azucar, D., Marengo, D., and Settanni, M. (2018). Predicting the big 5 personality traits from digital footprints on social media: A meta-analysis. *Personality and Individual Differences*, 124:150–159.
- [6] Bae, J. K. and Kim, J. (2015). A personal credit rating prediction model using data mining in smart ubiquitous environments. *International Journal of Distributed Sensor Networks*, 11(9):179060.
- [7] Bahulkar, A., Szymanski, B. K., Chan, K., and Lizardo, O. (2017). Coevolution of a multilayer node-aligned network whose layers represent different social relations. *Computational Social Networks*, 4.
- [8] Barabási, A.-L. and Pósfai, M. (2016). *Network science*. Cambridge university press.
- [9] Björkegren, D. and Grissen, D. (2017). Behavior revealed in mobile phone usage predicts loan repayment. *arXiv preprint arXiv:1712.05840*.
- [10] Blondel, V. D., Decuyper, A., and Krings, G. (2015). A survey of results on mobile phone datasets analysis. *EPJ Data Science*, 4(1):10.
- [11] Buettner, R. (2017). Predicting user behavior in electronic markets based on personality-mining in large online social networks. *Electronic Markets*, 27(3):247–265.
- [12] Castilho, D., de Melo, P. O. V., and Benevenuto, F. (2017). The strength of the work ties. *Information Sciences*, 375:155–170.
- [13] Chawla, N. V. (2009). Data mining for imbalanced datasets: An overview. In *Data mining and knowledge discovery handbook*, pages 875–886. Springer.
- [14] Chittaranjan, G., Blom, J., and Gatica-Perez, D. (2013). Mining large-scale smartphone data for personality studies. *Personal and Ubiquitous Computing*, 17(3):433–450.

- [15] Christy, A. J., Umamakeswari, A., Priyatharsini, L., and Neyaa, A. (2018). Rfm ranking—an effective approach to customer segmentation. *Journal of King Saud University-Computer and Information Sciences*.
- [16] Ciampi, F. (2015). Corporate governance characteristics and default prediction modeling for small enterprises. an empirical analysis of italian firms. *Journal of Business Research*, 68(5):1012–1025.
- [17] Clauset, A., Shalizi, C. R., and Newman, M. E. J. (2009). Power-Law Distributions in Empirical Data. *SIAM Review*, 51(4):661–703.
- [18] de Montjoye, Y.-A., Quoidbach, J., Robic, F., and Pentland, A. S. (2013a). Predicting personality using novel mobile phone-based metrics. In *International conference on social computing, behavioral-cultural modeling, and prediction*, pages 48–55. Springer.
- [19] de Montjoye, Y.-A., Quoidbach, J., Robic, F., and Pentland, S. (2013b). Predicting Personality Using Novel Mobile Phone-Based Metrics. In *SBP*, pages 48–55, Washington DC.
- [20] de Oliveira, R., Karatzoglou, A., Concejero Cerezo, P., Armenta Lopez de Vicuña, A., and Oliver, N. (2011). Towards a psychographic user model from mobile phone usage. In *CHI’11 Extended Abstracts on Human Factors in Computing Systems*, pages 2191–2196. ACM.
- [21] Doroz, R., Kudlacik, P., and Porwik, P. (2018). Online signature verification modeled by stability oriented reference signatures. *Information Sciences*.
- [22] Eagle, N. and Lazer, D. (2007). Inferring social network structure using mobile phone data [j]. *PNAS*.
- [23] Frias-Martinez, V., Virseda, J., and Frias-Martinez, E. (2010). Socio-economic levels and human mobility. In *Qual meets quant workshop-QMQ*.
- [24] Ge, R., Feng, J., Gu, B., and Zhang, P. (2017). Predicting and deterring default with social media information in peer-to-peer lending. *Journal of Management Information Systems*, 34(2):401–424.

- [25] Hadiji, F., Sifa, R., Drachen, A., Thureau, C., Kersting, K., and Bauckhage, C. (2014). Predicting player churn in the wild. In *Computational intelligence and games (CIG), 2014 IEEE conference on*, pages 1–8. IEEE.
- [26] Hu, J., Huang, L., Huang, J., Sun, T., and Ouyang, Y. (2017). What-if model construction and validation of web systems based on log mining. In *Asia-Pacific Software Engineering Conference (APSEC), 2017 24th*, pages 505–512. IEEE.
- [27] Hung, S.-Y., Yen, D. C., and Wang, H.-Y. (2006). Applying data mining to telecom churn management. *Expert Systems with Applications*, 31(3):515–524.
- [28] Husain, W. (2015). A study of customer behaviour through web mining. *Journal of Information Sciences and Computing Technologies*, 2(1):103–107.
- [29] Iglesias, J. A., Ledezma, A., Sanchis, A., and Angelov, P. (2017). Real-time recognition of calling pattern and behaviour of mobile phone users through anomaly detection and dynamically-evolving clustering. *Applied Sciences*, 7(8):798.
- [30] Johnson, J. W. (2000). A heuristic method for estimating the relative weight of predictor variables in multiple regression. *Multivariate behavioral research*, 35(1):1–19.
- [31] Klaus, A., Yu, S., and Plenz, D. (2011). Statistical Analyses Support Power Law Distributions Found in Neuronal Avalanches. *PLoS ONE*, 6(5):e19779.
- [32] Kovanen, L., Saramaki, J., and Kaski, K. (2011). Reciprocity of mobile phone calls. *Dynamics of Socio-Economic Systems*, 2(2):138–151.
- [33] Kuznetsova, N. V. and Bidyuk, P. I. (2017). Modeling of credit risks on the basis of the theory of survival. *Journal of Automation and Information Sciences*, 49(11).

- [34] Kvamme, H., Sellereite, N., Aas, K., and Sjørusen, S. (2018). Predicting mortgage default using convolutional neural networks. *Expert Systems with Applications*, 102:207–217.
- [35] Lambiotte, R., Blondel, V. D., de Kerchove, C., Huens, E., Prieur, C., Smoreda, Z., and Van Dooren, P. (2008). Geographical dispersal of mobile communication networks. *Physica A: Statistical Mechanics and its Applications*, 387(21):5317–5325.
- [36] LeBreton, J. M. and Tonidandel, S. (2008). Multivariate relative importance: Extending relative weight analysis to multivariate criterion spaces. *Journal of Applied Psychology*, 93(2):329.
- [37] Li, L., Li, A., Hao, B., Guan, Z., and Zhu, T. (2014a). Predicting active users’ personality based on micro-blogging behaviors. *PloS one*, 9(1):e84997.
- [38] Li, M.-X., Palchykov, V., Jiang, Z.-Q., Kaski, K., Kertész, J., Miccichè, S., Tumminello, M., Zhou, W.-X., and N Mantegna, R. (2014b). Statistically validated mobile communication networks: the evolution of motifs in European and Chinese data. *New Journal of Physics*, 16(8):083038.
- [39] Li, W., Li, X., Yao, M., Jiang, J., and Jin, Q. (2015). Personalized fitting recommendation based on support vector regression. *Human-centric computing and information sciences*, 5(1):21.
- [40] Lin, C., Xie, R., Guan, X., Li, L., and Li, T. (2014). Personalized news recommendation via implicit social experts. *Information Sciences*, 254:1–18.
- [41] Ling, R., Bertel, T. F., and Sundsøy, P. R. (2012). The socio-demographics of texting: An analysis of traffic data. *New Media & Society*, 14(2):281–298.
- [42] Liu, Y., Wang, J., and Jiang, Y. (2016a). Pt-lda: A latent variable model to predict personality traits of social network users. *Neurocomputing*, 210:155–163.

- [43] Liu, Z., Wang, Y., Mahmud, J., Akkiraju, R., Schoudt, J., Xu, A., and Donovan, B. (2016b). To buy or not to buy? understanding the role of personality traits in predicting consumer behaviors. In *International Conference on Social Informatics*, pages 337–346. Springer.
- [44] Luo, S., Morone, F., Sarraute, C., Travizano, M., and Makse, H. A. (2017). Inferring personal economic status from social network location. *Nature Communications*, 8:15227.
- [45] Ma, H., Jia, M., Zhang, D., and Lin, X. (2017). Combining tag correlation and user social relation for microblog recommendation. *Information Sciences*, 385:325–337.
- [46] Maldonado, S., Peters, G., and Weber, R. (2018). Credit scoring using three-way decisions with probabilistic rough sets. *Information Sciences*.
- [47] Mao, H., Shuai, X., Ahn, Y.-Y., and Bollen, J. (2013). Mobile communications reveal the regional economy in côte d’ivoire. *Proc. of NetMob*.
- [48] Martin, S., Nelson, B., Sewani, A., Chen, K., and Joseph, A. D. (2005). Analyzing behavioral features for email classification. In *CEAS*.
- [49] Newman, M. E. J. (2001). Scientific collaboration networks. II. Shortest paths, weighted networks, and centrality. *Physical Review E*, 64(1):016132.
- [50] Noh, G., Oh, H., and Lee, J. (2018). Power users are not always powerful: the effect of social trust clusters in recommender systems. *Information Sciences*.
- [51] Onnela, J.-P., Saramäki, J., Hyvönen, J., Szabó, G., Lazer, D., Kaski, K., Kertész, J., and Barabási, A.-L. (2007). Structure and tie strengths in mobile communication networks. *Proceedings of the National Academy of Sciences of the United States of America*, 104(18):7332–6.
- [52] Opsahl, T., Agneessens, F., and Skvoretz, J. (2010). Node centrality in weighted networks: Generalizing degree and shortest paths. *Social Networks*, 32(3):245–251.

- [53] Pan, W., Xia, S., Liu, Z., Peng, X., and Ming, Z. (2016). Mixed factorization for collaborative recommendation with heterogeneous explicit feedbacks. *Information Sciences*, 332:84–93.
- [54] Pearson, K. (1901). Liii. on lines and planes of closest fit to systems of points in space. *The London, Edinburgh, and Dublin Philosophical Magazine and Journal of Science*, 2(11):559–572.
- [55] Peska, L. and Vojtas, P. (2017). Using implicit preference relations to improve recommender systems. *Journal on Data Semantics*, 6(1):15–30.
- [56] Pratt, J. (1987). Dividing the indivisible using simple symmetry to partition variance explained. *Proceedings of the Second International Conference in Statistics*, pages 245–260.
- [57] Rochat, Y. (2009). Closeness centrality extended to unconnected graphs: The harmonic centrality index. In *ASNA*, number EPFL-CONF-200525.
- [58] San Pedro, J., Proserpio, D., and Oliver, N. (2015). Mobiscore: towards universal credit scoring from mobile phone data. In *International Conference on User Modeling, Adaptation, and Personalization*, pages 195–207. Springer.
- [59] Shields, A., Doody, P., and Scully, T. (2017). Application of multiple change point detection methods to large urban telecommunication networks. In *Signals and Systems Conference (ISSC), 2017 28th Irish*, pages 1–6. IEEE.
- [60] Singh, V. K., Freeman, L., Lepri, B., and Pentland, A. S. (2013a). Predicting Spending Behavior Using Socio-mobile Features. In *2013 International Conference on Social Computing*, pages 174–179. IEEE.
- [61] Singh, V. K., Freeman, L., Lepri, B., and Pentland, A. S. (2013b). Predicting spending behavior using socio-mobile features. In *2013 International Conference on Social Computing*, pages 174–179. IEEE.
- [62] Smith-Clarke, C., Mashhadi, A., and Capra, L. (2014). Poverty on the cheap: Estimating poverty maps using aggregated mobile communication

- networks. In *Proceedings of the SIGCHI Conference on Human Factors in Computing Systems*, pages 511–520. ACM.
- [63] Solenthaler, B., Klingler, S., Käser, T., and Gross, M. (2018). Ten years of research on intelligent educational games for learning spelling and mathematics. *arXiv preprint arXiv:1806.03257*.
- [64] Soto, V., Frias-Martinez, V., Virseda, J., and Frias-Martinez, E. (2011). Prediction of socioeconomic levels using cell phone records. In *International Conference on User Modeling, Adaptation, and Personalization*, pages 377–388. Springer.
- [65] Sun, J., Lang, J., Fujita, H., and Li, H. (2018). Imbalanced enterprise credit evaluation with dte-sbd: Decision tree ensemble based on smote and bagging with differentiated sampling rates. *Information Sciences*, 425:76–91.
- [66] Thomas, D. R., Hughes, E., and Zumbo, B. D. (1998). On variable importance in linear regression. *Social Indicators Research*, 45(1-3):253–275.
- [67] Thomas, D. R., Zhu, P., Zumbo, B. D., and Dutta, S. (2008). On measuring the relative importance of explanatory variables in a logistic regression. *Journal of Modern Applied Statistical Methods*, 7(1):4.
- [68] Thomas, D. R., Zumbo, B. D., Kwan, E., and Schweitzer, L. (2014). On johnson’s (2000) relative weights method for assessing variable importance: A reanalysis. *Multivariate behavioral research*, 49(4):329–338.
- [69] Tibshirani, R. (1996). Regression shrinkage and selection via the lasso. *Journal of the Royal Statistical Society. Series B (Methodological)*, pages 267–288.
- [70] Vapnik, V. N. (1999). An overview of statistical learning theory. *IEEE transactions on neural networks*, 10(5):988–999.
- [71] Wang, C., Lizardo, O., Hachen, D., Strathman, A., Toroczkai, Z., and Chawla, N. V. (2013). A dyadic reciprocity index for repeated interaction networks. *Network Science*, 1(1):31–48.

- [72] Wang, Y. and Lee, Y.-C. (2018). Customer credit evaluation using big data of microfinance company in china. *The Korean Academic Society of Business Administration*, (2):1601–1645.
- [73] Xiao, J., Jiang, X., He, C., and Teng, G. (2016). Churn prediction in customer relationship management via gmdh-based multiple classifiers ensemble. *IEEE Intelligent Systems*, 31(2):37–44.
- [74] Xie, J. and Szymanski, B. K. (2011). Community detection using a neighborhood strength driven label propagation algorithm. In *IEEE NSW 2011*, pages 188–195.
- [75] Xie, J., Szymanski, B. K., and Liu, X. (2011). Slpa: Uncovering overlapping communities in social networks via a speaker-listener interaction dynamic process. In *ICDM 2011 Workshop on DMCCI*.
- [76] Zhang, C., Zhang, H., and Wang, J. (2018). Personalized restaurant recommendation method combining group correlations and customer preferences. *Information Sciences*, 454:128–143.
- [77] Zhang, W., Du, Y., Yoshida, T., and Yang, Y. (2019). Deeprec: A deep neural network approach to recommendation with item embedding and weighted loss function. *Information Sciences*, 470:121–140.
- [78] Zhang, X.-j. and Hu, J. (2009). Personal credit rating assessment for the national student loans based on artificial neural network. In *Business Intelligence and Financial Engineering, 2009. BIFE'09. International Conference on*, pages 53–56. IEEE.
- [79] Zipf, G. and Behavior, H. (1950). The principle of least effort. *Reading, MA7 Addison Wesley*.

## Appendix A. Reciprocity Measures

Here we generalize how reciprocity is defined using  $R_i = \sum_j N_{i,j} r_{i,j}$  where  $r_{i,j}$  is the reciprocity score between node  $i$  and  $j$  and  $N_{i,j}$  is the weight of that

score. To keep the metric bounds at  $[-1, 1]$ , we constrain  $r_{i,j}$  to  $[-1, 1]$  and require  $N_{i,j}$  to be normalized, ( $1 = \sum_j N_{i,j}$ ). Previously, we defined a metric using  $r_{i,j} = \frac{w_{i,j} - w_{j,i}}{w_{i,j} + w_{j,i}}$  and where all scores are equal. Under normalization this means that  $N_{i,j} = \frac{1}{k_i}$  where  $k_i$  is the total degree of node  $i$ . Here we introduce two variants to produce two alternative metrics for reciprocity.

First we remove the dependence on the number of communications by modifying  $r_{i,j}$  to take on only three values  $-1, 0, 1$ , causing links with small  $w_{i,j}$  to become more important. If between node  $i$  and node  $j$  there exists any number of communications from  $i$  to  $j$ , but no communications from  $j$  to  $i$ , then  $r_{i,j} = 1$ . If the opposite is true, then  $r_{i,j} = -1$ . Finally if both  $i$  and  $j$  send any number of communications to each other,  $r_{i,j} = 0$ .  $N_{i,j}$  in this metric is unchanged. We call this metric binary weighted reciprocity.

The second metric modifies  $N_{i,j}$  rather than  $r_{i,j}$ . To make high volume links more important, we set  $N_{i,j} \propto w_{i,j} + w_{j,i}$ . Applying normalization leads to  $N_{i,j} = \frac{w_{i,j} + w_{j,i}}{\sum_{j'} w_{i,j'} + w_{j',i}}$ . The simplified expression is then  $R_i = \sum_j \frac{w_{i,j} - w_{j,i}}{\sum_{j'} w_{i,j'} + w_{j',i}}$ , which we call hyper-weighted reciprocity.

In Fig A.7, we show the distribution for both of these metrics. The hyper-weighted reciprocity is very similar to the weighted reciprocity, but the binary distribution is significantly different. Most of these difference arise from the binary nature of the metric, where for example a node with degree three can only have reciprocity  $0, \pm 1/3, \pm 2/3, \pm 1$ . Because the system is dominated by low degree nodes, this type of scenario is frequent causing a few discrete fractions to be most prevalent. Further, we include a fit following the same methodology as in Fig 3, where Table A.7 shows the fitting parameters.

Unfortunately, these features are not sufficiently unique from that shown in the main text of this work, and thus not suitable as separate features. The binary and weighted metrics have a Pearson correlation coefficient of 0.9224, while the hyper-weighted and weighted metrics have a coefficient of 0.727. Because of these high levels of correlation and despite weighting reciprocity differently, we conclude that the alternate methods do not produce any sufficiently unique information. They can, however, be substituted for the metric used based on

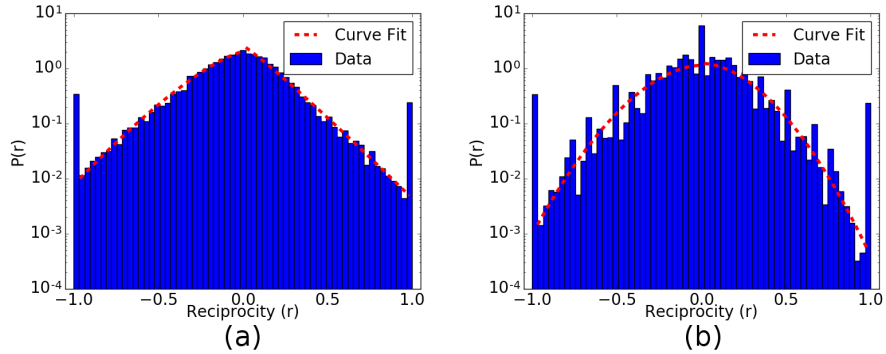


Figure A.7: (a) The distribution of reciprocities using the hyper-weighted metric. (b) The distribution of reciprocities using the binary metric. Both metrics maintain the extreme values. They also maintain a bell shape curve, but the binary metric exhibits multiple discrete peaks.

Fitting Parameter	Binary Weighted		Hyper-weighted	
	Positive	Negative	Positive	Negative
A	0.218	0.136	0.957	0.707
B	1.84	1.83	1.08	1,33
C	0.124	0.142	0.157	0.179
$R^2$	.798	0.785	0.957	.976

Table A.7: The fitting parameters used in Fig A.7. Positive and Negative refer to the fit of the distribution where the reciprocity values are positive and negative respectively. The Binary metric has relatively poor  $R^2$  values due to the many peaks present, but the fit captures the general shape. The Hyper-weighted metric performs better on goodness of fit and clearly shows the asymmetry between the positive and negative side of the distribution.

specific use cases where the intuition behind the calculations fits better, and thus may be useful for future work.

## Appendix B. Feature Sets

### Appendix B.1. Consumption features

Consumption features include information about the total number of communication events, the total and average duration of phone calls, and average time between consecutive communications. These broad categories are then

broken up into time windows (specific times of day or days of the week) and separated by communication type and direction to form a large contribution to our overall feature set. These features characterize the normal activity patterns for individuals within the network. On average, per day each user makes 5.3 calls lasting about 40 seconds each, and sends 10.4 messages. Additionally, this feature shows a slightly higher wait time for incoming events (3 hours) than outgoing events (2.5 hours).

#### *Appendix B.2. Correspondent features*

Correspondent features are based on the distinct number of individuals that each user communicates with over specific time periods, separated between calls and text messages. This includes the total number of unique people that exchange at least five messages with the user on average every week, and the number of regular correspondents that make at least two calls to the user on average in a week. Further, this feature includes the percentage of incoming communications that are messages and the number of unique correspondents over various time periods and scales (such as normal business hours versus rest hours and week days versus weekends). Analysis of this feature set shows that the average number of correspondents (call or message) is 31, while call correspondents make on average 21 calls and message correspondents sent on average 17 messages. However for regular correspondents, each user makes only 3.3 calls and sends 1.7 messages. The number of unique correspondents during the weekend drops to about half of the number for weekdays.

#### *Appendix B.3. Reciprocated event features*

We define reciprocated events as events where the observed user returns a call/message within an hour of receiving a communication. We extract this information for each user and every hour of the week, as well as the median time between reciprocated call events and median time to answer messages. Similar to above, we also aggregate these indicators to days of week and time of day. On average, this analysis shows that users reciprocate only 14 calls and 15

messages for the night time (midnight-6am) during the whole 3-month period. Interestingly, the average time to answer a message is only 21 minutes in the morning (6am-10am). This drops even further to a little less than 10 minutes during other times of the day (10am-6am). Further, the average number of reciprocated messages increases as the week goes by, going from 6.5 to 6.9 from Monday to Friday, but then dropping to 5.7 and 4.8 on Saturday and Sunday, respectively.

#### *Appendix B.4. Mobility features*

Mobility features describe daily movement patterns of a person. They use the cell tower location to which the individual connected to for each event. Features include average daily radius of gyration (minimum radius that encompasses all the locations visited by a user), average distance traveled per day of week (calculated as sum of distances between consecutive antennas), popular cell towers (IDs of most popular cell towers that sum up to 90% of records) and average number of unique cell towers per week. A typical user's average daily radius of gyration is 8.5 km. Interestingly, there is an order of magnitude difference when comparing mean and median distance traveled by day of the week, but the trend is the same in both cases. From Monday to Thursday, the median distance traveled is fairly constant around 33 km, but increases to 40 km on Friday and 47km on Saturday before dropping to 23 km on Sunday. Lastly, the average number of utilized cell towers per week is 15.

#### *Appendix B.5. Location features*

From information about the two most commonly used cell towers and the default status of each user, we can develop location features to identify high risk geographic regions. We use two cell towers instead of one to account for users spending a large amount of time at both their residence and workplace/school. For this reason, two new features are added for each user; one for each tower. From this information, we can calculate the empirical probability of default for each cell tower, yielding a mean of 0.0032. Note that when used for prediction

purposes, these calculations are based only on the training data set and then applied to the test dataset accordingly (more information on this experimental setting is in 6.1).